

# Specific features of single-pulse femtosecond laser micron and submicron ablation of a thin silver film coated with a micron-thick photoresist layer

D.A. Zayarnyi, A.A. Ionin, S.I. Kudryashov, S.V. Makarov, A.A. Rudenko, E.A. Drozdova, S.B. Odínokov

**Abstract.** Specific features of ablation of a thin silver film with a 1- $\mu\text{m}$ -thick layer of a highly transparent photoresist and the same film without a photoresist layer under single tightly focused femtosecond laser pulses in the visible range (515 nm) are experimentally investigated. Interference effects of internal modification of the photoresist layer, its spallation ablation from the film surface and formation of through hollow submicron channels in the resist without its spallation but with ablation of the silver film lying under the resist are found and discussed.

**Keywords:** thin silver film with a micron-thick layer of a transparent photoresist, femtosecond laser pulses in the visible range, tight focusing, submicron and micron ablation.

## 1. Introduction

Recently, femtosecond laser surface ablation has been widely investigated in view of the prospects of the precise treatment of surfaces of diverse materials (metals, semiconductors, insulators [1–3]), as well as the formation of nanoholes and detachment of nanoparticles during nanoscale ablation of thin films by single tightly focused ultrashort laser pulses (USLPs) [1, 4–8]. The corresponding physical mechanisms, cavitation formation of sub-100-nm holes [9, 10] and, apparently, somewhat smaller nanoparticles [8–10], as well as near- or supercritical phase explosion, under which larger (of submicron or micron sizes) holes and submicron nanoparticles are formed [11–13], were systematically investigated by varying the type of the film material and film thickness and laser energy density and duration. Similar results were obtained for both nano- and femtosecond laser pulses [9, 10, 12].

**D.A. Zayarnyi, A.A. Ionin, A.A. Rudenko** P.N. Lebedev Physics Institute, Russian Academy of Sciences, Leninsky prosp. 53, 119991 Moscow, Russia; e-mail: aion@sci.lebedev.ru;

**S.I. Kudryashov** P.N. Lebedev Physics Institute, Russian Academy of Sciences, Leninsky prosp. 53, 119991 Moscow, Russia; National Research Nuclear University ‘MEPhI’, Kashirskoe sh. 31, 115409 Moscow, Russia; e-mail: sikudr@sci.lebedev.ru;

**S.V. Makarov** P.N. Lebedev Physics Institute, Russian Academy of Sciences, Leninsky prosp. 53, 119991 Moscow, Russia; ITMO University, Kronverkskii prosp. 49, 197101 St. Petersburg, Russia; e-mail: makser@sci.lebedev.ru;

**E.A. Drozdova, S.B. Odínokov** N.E. Bauman Moscow State Technical University, 2-ya Baumanskaya ul. 5, 105005 Moscow, Russia; e-mail: odínokov@bmstu.ru

Received 22 February 2015  
Kvantovaya Elektronika 45 (5) 462–466 (2015)  
Translated by Yu.P. Sin’kov

At the same time, femtosecond laser ablation of the surface of materials coated with a thin layer of an optically transparent dielectric has been theoretically and experimentally investigated in the last years [14–16]. To date, only the spatial (mechanical) limitation of surface ablation by a dielectric layer has been considered theoretically [14, 15]. However, experiments revealed another important physical effect: self-focusing and filamentation of focused USLPs with a supercritical peak power in a thin (millimetre) dielectric layer [16]. Moreover, transparent dielectrics allow for implementing filamentation on the micron scale under tightly focused USLPs with supercritical peak powers [17]. In particular, hollow ablation channels of submicron diameter and micron length were observed on the surface of fused silica exposed to tightly focused USLPs even at subcritical peak powers [18].

In addition, previous studies with longer (nanosecond) laser pulses revealed also optical interference in submicron transparent films, which significantly affects the power transfer to the material surface, depending on the film thickness [19], and the surface boiling of submicron liquid dielectric film, with its subsequent detachment; the characteristics of the latter process (detachment time, velocity, etc.) are size-dependent [20–23]. Similar ablation effects via detachment (spallation ablation of a liquid layer [24]) were experimentally observed only in [25], where a silicon surface with a (20–1200)-nm-thick oxide layer was exposed to USLPs. Thus, there are only few fundamental experiments in the field of ablation of targets with a thin dielectric layer under focused USLPs, which yield a very fragmentary phenomenological pattern of this phenomenon [in contrast to the numerous studies on thicker (multimicron) and more transparent (generally liquid) films].

In this paper, we report the results of experimental study of the specific features of single-pulse femtosecond laser ablation of the surface of a thin silver film coated by a micron-thick layer of a transparent photoresist, under variable focusing conditions and power characteristics of USLPs, which suggest microscale filamentation of the laser beam in the photoresist layer and the corresponding effects of submicron ablation of the metal film under this layer. We were interested in both direct submicron ablation of the film through the resist layer or its ablation by a filamented laser beam and the formation of through channels in the photoresist layer (even in the absence of film ablation) as a result of its direct or filamentation ablation, as well as in the photolithographic version: after laser or filamentation exposure of the photoresist with its subsequent chemical development.

## 2. Experimental

Silver films 50–55 nm in thickness were deposited on silicate object glasses in the form of 2-mm-thick plates, 20 mm long and wide, cleaned in an ultrasonic bath. The film growth was performed in a Luch-013 magnetron system for depositing protective and decorative coatings. Positive photoresist Microposit S-1813 was deposited on the silver film surface on a centrifuge in the form of a homogeneous, optically transparent layer 1–1.1  $\mu\text{m}$  thick [26]; some samples were not coated with the resist to be used as references.

Single-pulse laser irradiation of each sample, mounted on a computer-controlled motorised table, was performed in a trinocular optical microscope, using the optical visualisation channel. The exposure region was visualised using the ocular chamber in the microscope binocular unit. Specimens were exposed to USLPs generated by an ytterbium-doped Satsuma fibre laser (Amplitude Systemes), with a centre wavelength of  $\sim 1030$  nm, pulse width (FWHM)  $\sim 0.3$  ps, and energy per pulse of about 8  $\mu\text{J}$  ( $\text{TEM}_{00}$  mode,  $M^2 \approx 1.05$ ). The pulses were frequency-doubled in a thin BBO crystal; USLPs in the visible range (515 nm) with FWHM  $\sim 0.2$  ps and energy up to 3  $\mu\text{J}$  were selected by a dichroic mirror. Second-harmonic pulses were focused by micro-lenses with numerical aperture values  $\text{NA} = 0.1, 0.25$  and  $0.65$  (with aperture filled) into focal spots with diameters  $D_{1/e} \approx 2.4, 0.9$  and  $0.3$   $\mu\text{m}$ . The target surface was irradiated by pulses in the scan regime; the pulse repetition rate was  $f \approx 1$  Hz and the scan rate was  $V \sim 3$   $\mu\text{m s}^{-1}$ . The exposed samples were developed using Microposit 303 with subsequent rinsing in deionised water and drying in a jet of squeezed air. Samples were visualised in a JEOL 7001F scanning electron microscope (SEM).

## 3. Results and discussion

### 3.1. Test ablation of a silver film without a resist

Test ablation of a silver film without a resist layer was carried out to estimate the threshold energy density necessary for ablating a film of this thickness with formation of a hole at different NA values of the focusing optics. The estimation was performed on the assumption of the existing dimensional effect of USLP energy transfer with allowance for lateral thermal conductivity [10]. A series of linear arrays of holes was recorded for each NA value at different USLP energies (Fig. 1), after which the standard formula for the energy density distribution in a Gaussian beam was used to determine the threshold values of effective energy density  $F_{\text{hole}}$  and effective ‘thermal’  $1/e$  diameters  $W_{1/e}$  of the temperature field on the hole-formation scales [27]. The thresholds  $F_{\text{hole}}$  were  $0.7 \pm 0.2$   $\text{J cm}^{-2}$  (the threshold values of the incident energy density were 17, 8 and 3  $\text{J cm}^{-2}$  for  $\text{NA} = 0.65, 0.25$  and  $0.1$ , respectively) with a spread of effective values  $W_{1/e}$  from 1.5 ( $\text{NA} = 0.65$ ) to 2.8 ( $\text{NA} = 0.25$ ) and 5 ( $\text{NA} = 0.1$ )  $\mu\text{m}$ , which always exceeded the corresponding focal diameter  $D_{1/e}$  by 1.5–2.5  $\mu\text{m}$ , a value determining the scale of lateral heat transfer at times necessary for hole formation [9–12]. Along with holes, we also observed a series of intermediate low-energy nanostructures, such as nanohills and developing nanotips (Fig. 2), with effective formation thresholds in the range of  $0.5$ – $0.7$   $\text{J cm}^{-2}$ .

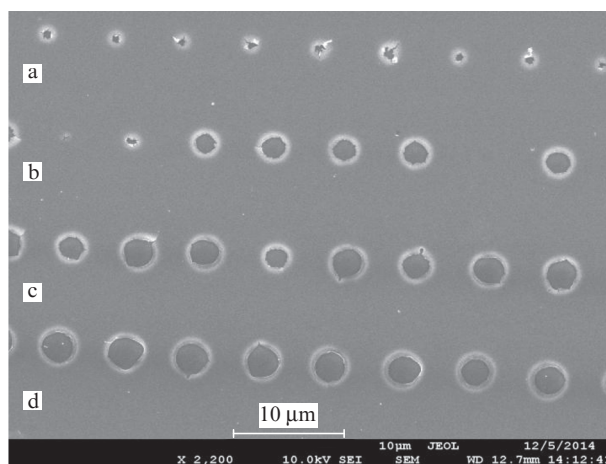


**Figure 1.** SEM image of arrays of ablation holes on the surface of a silver film without a resist layer, formed at  $\text{NA} = 0.25$  and USLP energies of (a) 25, (b) 30, (c) 35 and (d) 50 nJ.

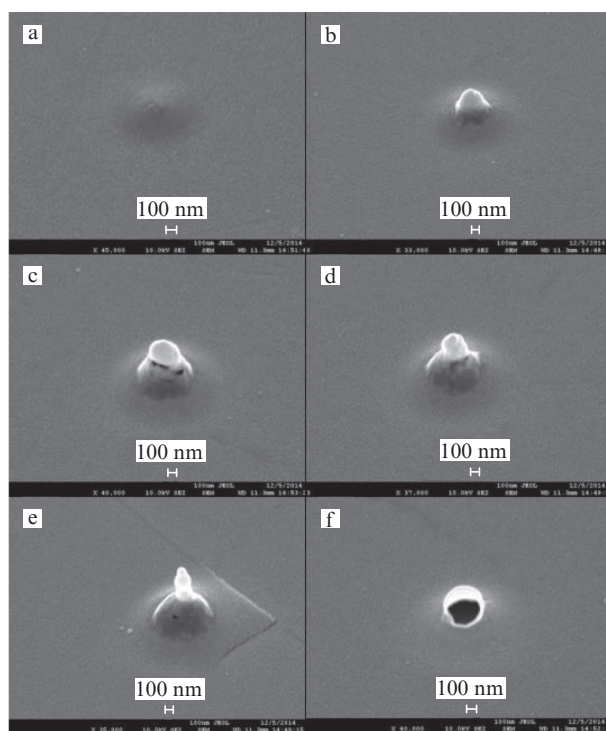


**Figure 2.** SEM images (recorded at an angle of  $40^\circ$ ) of individual nanoelements, formed on the surface of a silver film without a resist layer at  $\text{NA} = 0.65$  and USLP energies of (a) 12, (b) 14, (c) 15, (d) 16, (e) 17 and (f) 19 nJ.

### 3.2. USLP interference in the resist film

The high quality of the photoresist layer (high homogeneity and transparency) was confirmed experimentally: we observed high-contrast interference peaks between an incident USLP (wave packet 60–70  $\mu\text{m}$  long in air) and its replica, reflected from the surface of a highly reflecting silver film, which formed a standing wave in the resist layer and in the air near the sample, as was suggested in [28]. Irradiation by tightly focused USLPs with lowest energies led to spallation ablation of the upper disk about 0.15  $\mu\text{m}$  thick from the photoresist layer (Fig. 3a), according to the first (from

the air/resist interface) interference maximum, the position of which ( $d_1 \approx 0.16 \mu\text{m}$ ) can be compared with the calculated position of the  $m$ th interference peak,  $d_m$ , in accordance with the interference condition  $d_m = m(\lambda/2n)$ , where  $\lambda$  is the USLP wavelength and  $n \approx 1.6$  is the refractive index of photoresist in the visible region.

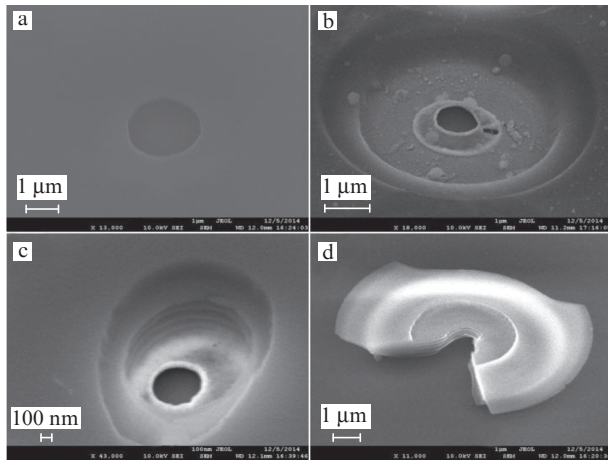


**Figure 3.** SEM images (recorded at an angle of  $40^\circ$ ) of (a–c) step craters on the surface of resist and (d) a layered spallation disk with an interference structure, formed on the surface of a silver film at  $\text{NA} = 0.65$ .

At high energies we observed spallation of the entire resist layer in the centre of the focal spot, whereas the spallation closer to the periphery was partial: approximately at the half-thickness level (Fig. 3b). In some cases, in correspondence with the dynamic interference pattern (Fig. 3c), the spallation of the remaining part was stepwise. The wall stratification observed in this case indicated the absence of a lateral exposed halo because of the optical nonlinearity of resist modification (in particular, it was expected to be two-photon for the Microposit S-1813 photoresist). Finally, the spallation disk also had a layered structure (Fig. 3d); the periodicity of the arrangement of brighter photomodification layers was consistent with the aforementioned interference condition. Note that interference was observed more clearly in the case of tight USLP focusing, which provided higher laser beam intensities, necessary for modification and partial spallation of the resist layer.

### 3.3. Spallation and strain of resist microdisks

Although the energy introduced into a silver film should be sensitive to the interference in the resist layer [19], statistical measurements on arrays of craters, where incomplete spallations randomly manifest themselves, make it possible to estimate the threshold energy densities necessary for complete thermomechanical spallation of resist disks almost without their ablation damage (Fig. 4). The corresponding threshold incident energy densities (disregarding lateral heat transfer) are as follows: 0.3, 3 and  $8 \text{ J cm}^{-2}$  (with allowance for transfer, the introduced energy density is  $0.04 \text{ J cm}^{-2}$  over) for  $\text{NA} = 0.1$ , 0.25 and 0.65, respectively. The disk removal times were few nanoseconds or even longer, because both nanotips and nanohills (which are known to be formed during few nanoseconds [9–12, 29]) are imprinted on the bottom side of disks (Fig. 4), a circumstance indicative of thermomechanical character of spallation of resist microdisks. It

is noteworthy that, under conditions of tight focusing ( $\text{NA} = 0.25$  and  $0.65$ ), resist ablation may occur in the absence of spallation (Figs 4b, 4d) and result in the formation of a hollow channel along the laser beam waist or filament; as shows the morphology of these submicron channels and the ablation products redeposited around it, this process will occur most likely in the fragmentation regime [24]. Apparently, specifically under tight focusing ( $\text{NA} = 0.25$  and  $0.65$ ), the USLP energy is sufficiently high to provide photoresist ablation (energy densities of 3 and  $8 \text{ J cm}^{-2}$ , respectively); however, it is insufficient for spallation of microdisks in view of insufficiently strong heating of the lower lying silver film because of the lateral heat transfer.

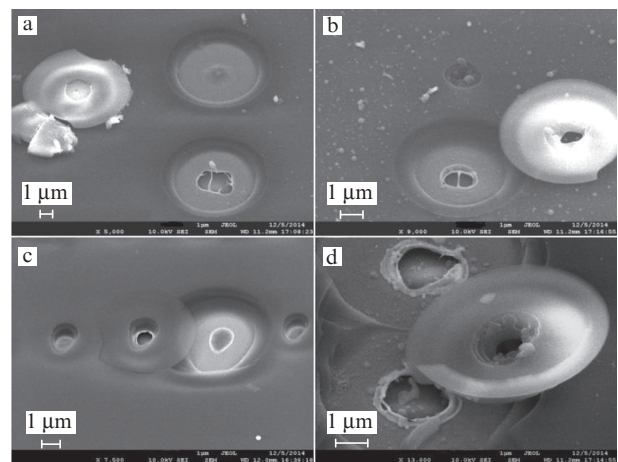


**Figure 4.** SEM images (recorded at an angle of  $40^\circ$ ) of the surface of a silver film with (a–d) complete and (b, c) incomplete removal of spallation disks of the resist under USLPs with  $\text{NA} =$  (a, c, d) 0.25 and (b) 0.65.

### 3.4. Ablation of a silver film with resist spallation

When the threshold of resist spallation ablation is overcome (in the range of energy densities of  $0.3\text{--}0.5 \text{ J cm}^{-2}$  for  $\text{NA} = 0.1$ ), cavitation nanoholes and ablation microholes, as well as intermediate evaporative structures (nanohills and nanotips)

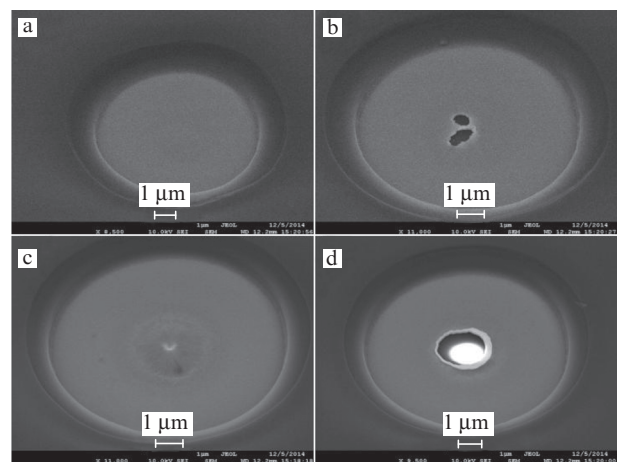


**Figure 5.** SEM images (recorded at an angle of  $40^\circ$ ) of craters in a resist layer with traces of ablation of a lower lying silver film at  $\text{NA} = 0.1$  and USLP energies of (a) 30, (b) 32, (c) 35 and (d) 37 nJ.



are formed in the film (Fig. 5). It is noteworthy that the presence of the resist facilitates their formation, because the corresponding thresholds in the incident energy density are lower in this case than for a film without a resist layer ( $3 \text{ J cm}^{-2}$ ). This can be caused by the antireflection interference effect in the resist layer, similar to that investigated previously in liquid films [19], and mechanical suppression of thermionic emission, ultrafast laser-plasma film ablation [30] and strong evaporative cooling effects [31, 32].

At the same time, even in the case of USLPs with sub-megawatt peak powers, one cannot exclude filamentation effects in the photoresist layer for tightly focused high-intensity USLPs, because the critical power, which generally amounts to several megawatts [16–18], rapidly decreases with decreasing USLP wavelength [33]. Correspondingly, the effective energy density in a possible filament may significantly exceed the moderate values of the energy density incident on the layer ( $0.3\text{--}0.5 \text{ J cm}^{-2}$ ). A significant decrease in the USLP ablation threshold of a material under a layer of a transparent liquid dielectric was noted in [34].

A more accurate choice of ablation conditions (to make the USLP energy closer to threshold) allows one to form holes up to 100 nm in diameter in the film (Fig. 6), even in the case of soft focusing ( $\text{NA} = 0.1$ ); this possibility was previously noted for free films [9, 10]. It was assigned to the formation of a narrow melt bath, in which nanoscale boiling spontaneously occurs with ejection of film fragments above expanding nanobubbles (spallation nanoablation). The spontaneous character of this process is observed, as for free films [10], in the form of multiple (for example, paired, see Fig. 6d) nanoholes arising in the film.

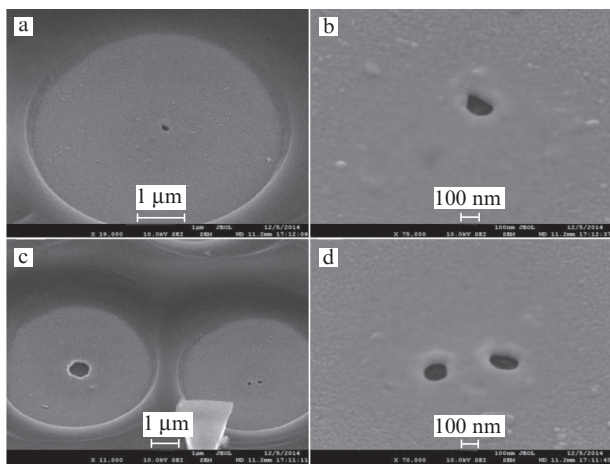


**Figure 6.** SEM images (recorded at an angle of  $40^\circ$ ) of craters in a resist layer with traces of ablation of a lower lying silver film at  $\text{NA} = 0.25$  and USLP energies of (a, b) 18 and (c, d) 20 nJ.

### 3.5. Ablation and manifestation of through hollow submicron channels without resist spallation

Hollow and non-hollow through modification channels were formed in the resist layer under the tightest focusing conditions ( $\text{NA} = 0.65$ ) by direct ablation of the resist, involving the silver film (Fig. 7a), at an incident energy density of  $8 \text{ J cm}^{-2}$  (Figs 7a–7c), i.e., near the spallation threshold for photoresist microdisks (see also Subsection 3.3 and Fig. 4). At the same time, in the case of ablation at an energy density

of  $9 \text{ J cm}^{-2}$ , the channels are much wider (up to  $1 \mu\text{m}$  in diameter), and ablation of the lower lying film is observed (Fig. 7d), which can be related both to additional photomodification, which manifests itself under chemical development, and to the large excess above the ablation threshold for the photoresist.

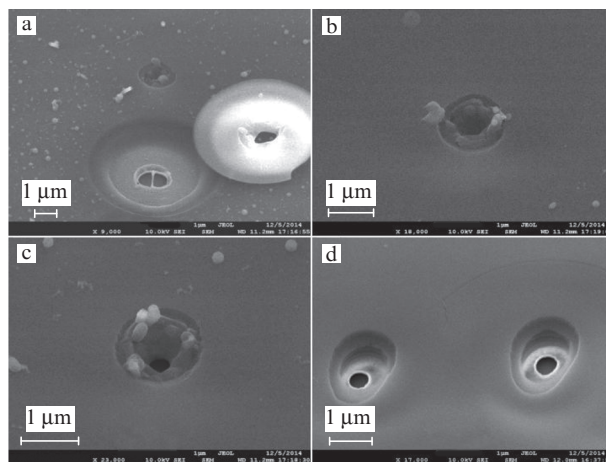


**Figure 7.** SEM images (recorded at an angle of  $40^\circ$ ) of channels in a resist layer at  $\text{NA} = 0.65$  and USLP energies of (a–c) 9 and (d) 10 nJ.

Note that, under these focusing conditions and at energy density below  $9 \text{ J cm}^{-2}$ , through channels were not observed after developing the exposed resist. This nontrivial fact can be explained, in particular, by the higher threshold of critical exposure of the resist layer, caused by the energy-consuming destruction of a large number of strong bonds, comparable with the number of monomers, whereas thermal fragmentation ablation of the resist may occur with direct ejection of large fragments. At the same time, one can use single-pulse exposure with an energy density not higher than  $9 \text{ J cm}^{-2}$  and choose the chemical development time such as to remove only a layer  $\sim 0.1 \mu\text{m}$  deep (see channel broadening in Figs 7b–7d) during development. Such a thin layer is insignificant for forming a pronounced channel in a resist layer  $1 \mu\text{m}$  thick; moreover, it is invisible on the resist surface. This issue is proposed to be investigated in more detail.

## 4. Conclusions

The comparative experimental study of ablation of a thin silver film with a layer of a highly transparent  $1\text{-}\mu\text{m}$ -thick photoresist and a film without this layer, exposed to single tightly focused femtosecond laser pulses in the visible range, revealed a number of interesting effects: interference and internal modification in the photoresist layer, its thermoelastic spallation ablation from the film surface, formation of fragmentation-ablation through hollow channels of submicron sizes in the resist without its spallation but with ablation of the lower lying silver film and a decrease in the formation threshold of nanostructures and microholes in the film coated with a resist. Along with further clarification experiments, the results obtained are proposed to be used for optimising the technology of more complex plasmonic nanostructures, in particular, hyperbolic metamaterials of optical and IR ranges in the form of arrays of metal nanorods in dielectric matrices.

**Acknowledgements.** This work was supported in part by the Russian Foundation for Basic Research (Grant No. 13-02-00971-a) and a programme of the Presidium of the Russian Academy of Sciences.

S.V. Makarov acknowledges the State Support of the Leading Universities of the Russian Federation (Grant No. 074-U01) within the ITMO Post-Doctoral Fellowship Programme.

## References

1. Preuss S., Spath M., Zhang Y., Stuke M. *Appl. Phys. Lett.*, **62**, 3049 (1993).
2. Pronko P.P., Dutta S.K., Squier J., Rudd J.V., Du D., Mourou G. *Opt. Commun.*, **114**, 106 (1995).
3. Korte F., Serbin J., Koch J., Egbert A., Fallnich C., Ostendorf A., Chichkov B.N. *Appl. Phys. A*, **77**, 229 (2003).
4. Koch J., Korte F., Bauer T., Fallnich C., Ostendorf A., Chichkov B.N. *Appl. Phys. A*, **81**, 325 (2005).
5. Nakata Y., Miyanaga N., Okada T. *Appl. Surf. Sci.*, **253**, 6555 (2007).
6. Kuznetsov A.I., Koch J., Chichkov B.N. *Appl. Phys. A*, **94**, 221 (2009).
7. Guo Z., Feng J., Zhou K., Xiao Y., Qu S., Lee J.-H. *Appl. Phys. A*, **108**, 639 (2012).
8. Kuznetsov A.I., Evlyukhin A.B., Gonçalves M.R., Reinhardt C., Koroleva A., Arnedillo M., Kiyan R., Marti O., Chichkov B.N. *ASC Nano*, **5**, 4843 (2011).
9. Kulchin Yu.N., Vitrik O.B., Kuchmizhak A.A., Nepomnyashchii A.V., Savchuk A.G., Ionin A.A., Kudryashov S.I., Makarov S.V. *Opt. Lett.*, **38**, 1452 (2013).
10. Danilov P.A., Drozdova E.A., Ionin A.A., Kudryashov S.I., Odinkov S.B., Rudenko A.A., Yurovskikh V.I., Zayarnyi D.A. *Appl. Phys. A*, **117**, 981 (2014).
11. Kulchin Yu.N., Vitrik O.B., Kuchmizhak A.A., Savchuk A.G., Nepomnyashchii A.A., Danilov P.A., Zayarnyi D.A., Ionin A.A., Kudryashov S.I., Makarov S.V., Rudenko A.A., Yurovskikh V.I., Samokhin A.A. *Zh. Eksp. Teor. Fiz.*, **146**, 21 (2014).
12. Danilov P.A., Zayarnyi D.A., Ionin A.A., Kudryashov S.I., Makarov S.V., Rudenko A.A., Yurovskikh V.I., Kulchin Yu.N., Vitrik O.B., Kuchmizhak A.A., Drozdova E.A., Odinkov S.B. *Kvantovaya Elektron.*, **44**, 540 (2014) [*Quantum Electron.*, **44**, 540 (2014)].
13. Emel'yanov V.I., Zayarnyi D.A., Ionin A.A., Kiseleva I.V., Kudryashov S.I., Makarov S.V., Rudenko A.A., Nguen Ch.T.Kh. *Pis'ma Zh. Eksp. Teor. Fiz.*, **99**, 601 (2014).
14. Upadhyay A.K., Inogamov N.A., Rethfeld B., Urbassek H.M. *Phys. Rev. B*, **78**, 045437 (2008).
15. Karim E.T., Shugaev M., Wu C., Lin Z., Hainsey R.F., Zhigilei L.V. *J. Appl. Phys.*, **115**, 183501 (2014).
16. Ionin A.A., Kudryashov S.I., Makarov S.V., Rudenko A.A., Saltuganov P.N., Seleznev L.V., Sunchugasheva E.S. *Appl. Surf. Sci.*, **292**, 678 (2014).
17. Couairon A., Sudrie L., Franco M., Prade B., Mysyrowicz A. *Phys. Rev. B*, **71**, 125435 (2005).
18. Kudryashov S.I., Joglekar A., Mourou G., Herbstman J.F., Hunt A.J. *Appl. Phys. Lett.*, **91**, 141111 (2007).
19. Kudryashov S.I., Allen S.D. *J. Appl. Phys.*, **95**, 5820 (2004).
20. Kudryashov S.I., Allen S.D. *J. Appl. Phys.*, **93**, 4306 (2003).
21. Kudryashov S.I., Allen S.D. *Appl. Phys. A*, **79**, 1737 (2004).
22. Kudryashov S.I., Lyon K., Shukla S., Murry D., Allen S.D. *J. Appl. Phys.*, **100**, 056103 (2006).
23. Kudryashov S.I., Allen S.D. *J. Appl. Phys.*, **100**, 104908 (2006).
24. Ionin A.A., Kudryashov S.I., Seleznev L.V., Sinitsyn D.V., Bunkin A.F., Lednev V.N., Pershin S.M. *Zh. Eksp. Teor. Fiz.*, **143**, 403 (2013).
25. McDonald J.P., Nees J.A., Yalisove S.M. *J. Appl. Phys.*, **102**, 063109 (2007).
26. Sagatelyan G.R., Odinkov S.B., Kuznetsov A.S., Drozdova E.A., Solomashenko A.B., Zherdev A.Yu., Donchenko S.S., Nikolaev V.V. *Nauchn. Obozr.*, **12**, 183 (2013).
27. Liu J.M. *Opt. Lett.*, **7**, 196 (1982).
28. Bulgakova N.M., Zhukov V.P., Vorobyev A.Y., Guo C. *Appl. Phys. A*, **92**, 883 (2008).
29. Unger C., Koch J., Overmeyer L., Chichkov B.N. *Opt. Express*, **20**, 24864 (2012).
30. Ionin A.A., Kudryashov S.I., Makarov S.V., Seleznev L.V., Sinitsyn D.V. *Appl. Phys. A*, **117**, 1757 (2014).
31. Ionin A.A., Kudryashov S.I., Makarov S.V., Saltuganov P.N., Seleznev L.V., Sinitsyn D.V. *Pis'ma Zh. Eksp. Teor. Fiz.*, **101** (5), 336 (2015).
32. Zayarnyi D.A., Ionin A.A., Kudryashov S.I., Makarov S.V., Rudenko A.A., Bezhanov S.G., Uryupin S.A., Kanavin A.P., Emel'yanov V.I., Alferov S.V., Khonina S.N., Karpeev S.V., Kuchmizhak A.A., Vitrik O.B., Kulchin Yu.N. *Pis'ma Zh. Eksp. Teor. Fiz.*, **101** (6), 428 (2015).
33. Fedorov V.Yu., Kandidov V.P. *Laser Phys.*, **18**, 1530 (2008).
34. Ren J., Kelly M., Hesselink L. *Opt. Lett.*, **30**, 1740 (2005).